

Velocity Structure Beneath the Eastern Offshore Region of Southern Taiwan Based on OBS Data

Allen T. Chen¹ and Yosio Nakamura²

(Manuscript received 13 March 1998, in final form 28 August 1998)

ABSTRACT

Six ocean bottom seismographs (OBSs) were deployed along an east-west seismic line at 22°12' N latitude in the eastern offshore region of southern Taiwan to record air-gun shots over the instruments. The line extends from 122°00'E in the Philippine Sea Basin to 120°55'E near the Hengchun Peninsula and crossed the North Luzon Arc, the North Luzon Trough, the Huatung Ridge and the Southern Longitudinal Trough, from east to west. A seismic velocity model along the profile derived from the acquired data includes two layers of sediments with a P-wave velocity of less than 3.6 km/s and upper and lower crusts with velocities of up to 5.3 km/s and 7.0 km/s, respectively. The sediment layer is very thin on the North Luzon Arc and Trough, but is as thick as 5 km under the Huatung Ridge and the Southern Longitudinal Trough. The crust, which is about 6 km thick under the Philippine Sea Basin, thickens westward and is more than 15 km under the North Luzon Arc and again towards the Hengchun Peninsula, with corresponding variations in Moho depth. The seismic structure in the area is thus consistent with a hypothesis that once a trench located along the Southern Longitudinal Trough might retreat farther west at a later stage.

(Key words: Offshore Taiwan, OBS, Velocity model)

1. INTRODUCTION

Seismic velocity structure in the area extends from the Manila Trench to the North Luzon Arc south of Taiwan is important for understanding the process of collision of the arc against the Eurasian continent. Tomographic studies to derive 3-D velocity structures based on earthquake data have provided only a crude velocity distribution in a grid mesh of wide (25-50 km) horizontal spacing beneath the island (Roecker *et al.*, 1987; Rau and Wu, 1995; Ma, *et al.*, 1996) with severely limited resolution in the offshore areas because of the increasing uncertainty in offshore earthquake locations as the seismic stations are mainly confined to land. A more direct approach relying on the use of ocean bottom seismographs (OBSs) was initiated early

¹Institute of Applied Geophysics, National Taiwan Ocean University, Keelung, Taiwan 202, ROC

²Institute for Geophysics, University of Texas at Austin, 4412 Spicewood Springs Road, Bldg. 600, Austin, Texas 78759-8500, USA

this decade (Chen and Nakamura, 1992; Chen *et al.*, 1994; Chen and Jaw, 1996), and was expanded during the Sino-U.S. deep seismic imaging study of the Taiwan arc-continent collision with a joint experiment in August and September of 1995. A part of this experiment was an OBS survey along a line straddling Hengchun Peninsula, roughly perpendicular to the local structural trend. This paper reports on processing, analysis and interpretation of the data from six OBSs along the eastern half of the line (Line 29, Figure 1). A companion paper by Nakamura, *et al.* (1998) describes the results from the western half of the line (Line 33).

2. TECTONIC SETTING

The collision between the Northern Luzon Arc and the Asian continent started in the late Neogene and has since been propagating southward as the Philippine Sea Plate continues to move northwestwards (Ho, 1982; Huang *et al.*, 1992). The Taitung Longitudinal Valley represents the suture zone of the collision with a part of the Northern Luzon Arc being accreted to Taiwan as the narrow, elongated Coastal Range (Figure 2). The suture zone extends southward and becomes the Southern Longitudinal Trough, while the Northern Luzon Arc continues to collide with the island. Currently situated between the Southern Longitudinal Trough and the Northern Luzon Arc are the Huatung Ridge and the Taitung Trough, while the Hengchun Peninsula abuts immediately to the west of the Southern Longitudinal Trough. The Taitung Trough may be considered as the northward extension of the North Luzon Trough, a forearc basin. Line 29 crosses these features from east to west. The Hengchun Ridge and at least a

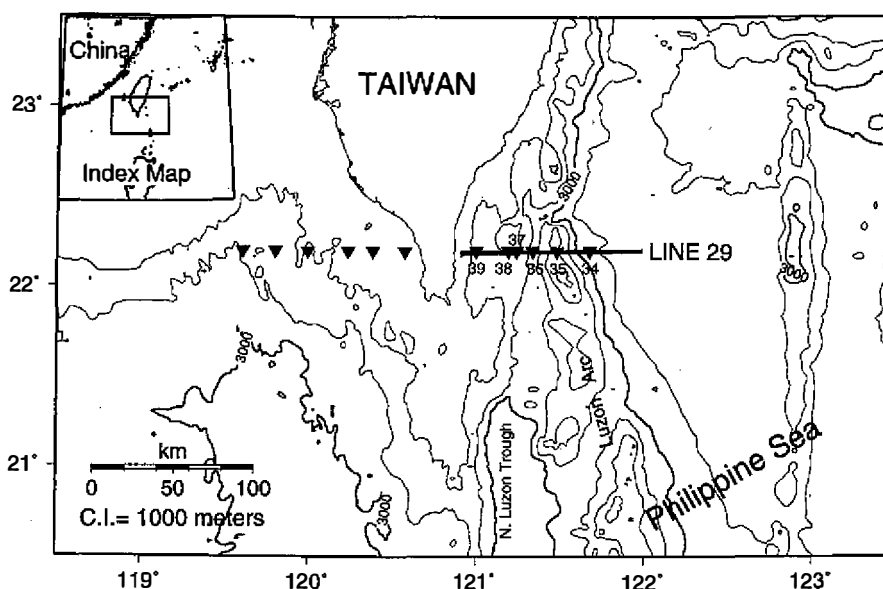


Fig. 1. Seismic Line 29 with locations of OBS nos. 34-39 in eastern offshore Hengchun Peninsula. Also shown are locations of OBS nos. 40-45 of Line 33 in western offshore region.

part of the Hengchun Peninsula are the accretionary block formed as the Asian continent subducted beneath the Manila Trench (Huang *et al.*, 1992, 1997).

The existence of strike slip components along the Taitung Longitudinal Valley (e.g. Chen, 1991; Cheng and Yeh, 1991; Angelier *et al.*, 1997) reflects the nature of oblique collision being associated with the Taitung Longitudinal Valley (Teng, 1991; Lee *et al.*, 1997; Fuh *et al.*, 1997; Hu *et al.*, 1997; Yu *et al.*, 1997). The collisional suture zone is a former subduction zone, whose southern extension is the relic of an ancient trench (Chai, 1972). The region between the North Luzon Trough and the Southern Longitudinal Trough, the Huatung Ridge, may represent a subduction melange developed in the west of the forearc basin, the North Luzon Trough (Huang *et al.*, 1992).

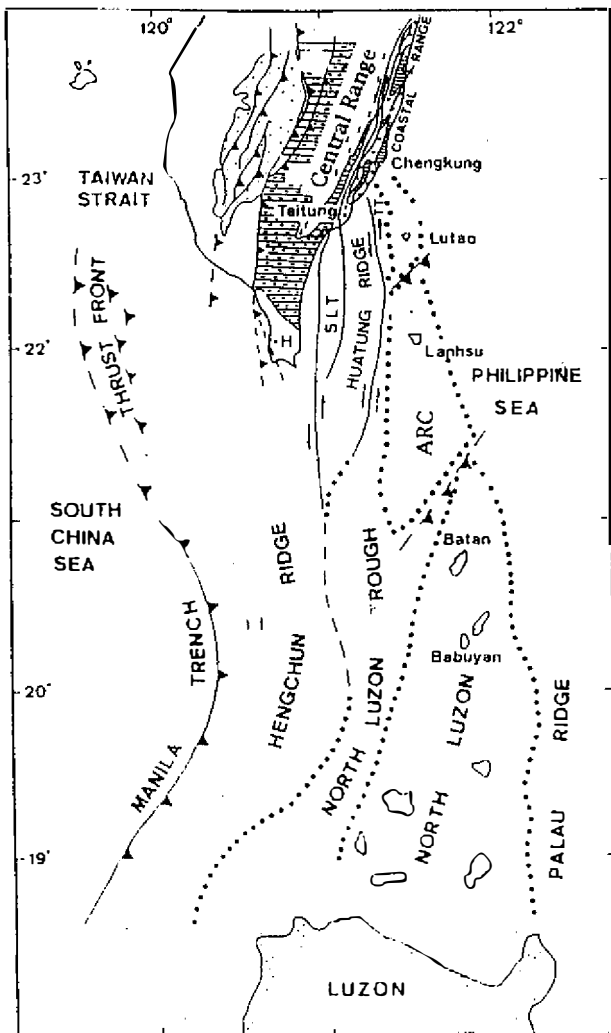


Fig. 2. Tectonic setting offshore from southern Taiwan after Huang *et al.* (1992), where from the north TT=Taitung Trough, SLT=Southern Longitudinal Trough, and H= Hengchun Peninsula.

3. DATA

As a part of the Sino-U.S. program for a deep seismic imaging of Taiwan arc-continent collision, six ocean bottom seismographs (OBSs) from the Institute for Geophysics at the University of Texas at Austin (UTIG) (Nakamura and Garmany, 1991) and National Taiwan Ocean University (NTOU) (Chen *et al.*, 1994) were deployed at Stations 34-39. These acquired wide-angle seismic data along the 112.4 km-long Line 29 which essentially followed the 22° 12' N latitude approximately perpendicular to the eastern coastline of the Hengchun Peninsula (Figure 1). The survey, of which the above line was a part, was a joint operation involving *R/V Ocean Researcher I*, Cruise No. 429, and *R/V Maurice Ewing*, Cruise No. 9509, and took place between August 24 and September 13, 1995.

A 135.8 l (8285 cu. in.) air-gun array towed by the *R/V Maurice Ewing* at a depth of 7 m below sea level, provided the seismic source for the experiment. The seismic signals generated were recorded simultaneously on a 3 km long streamer towed behind the *Maurice Ewing* and on the OBSs deployed by the *Ocean Researcher I*. Each OBS was equipped with three geophones, while an additional hydrophone was installed on each UTIG unit. After retrieval of each instrument, data recorded on a 1.215 GB disk were copied to a tape, examined on board, and taken back to respective labs in Austin and Keelung for further processing.

Signals from shots along Line 29 were discernible at the OBS stations only up to about 75 km, and these are the sole OBS data sets used in this paper. Although these same signals were also discernible at some of the Line 33 OBS stations in the western offshore region across the peninsula at distances beyond 100 km, with some of the Line 29 stations also recording signals from shots on Line 33, we defer the use of these data until a later study when the combined data from both lines will be analyzed.

4. PROCESSING AND ANALYSIS

We processed the data mainly by using software packages OBSTOOL (Christeson, 1995) and SIOSEIS (Henkart, 1980). In the initial step of the processing, we combined the raw OBS data with other auxiliary data sets such as clock calibrations, shot times, bathymetry, and differential GPS (DGPS) navigation to generate OBS data files in standard SEG-Y format (Nakamura, 1994; Chen and Jaw, 1996).

The location of each OBS on the sea floor (Table 1) was computed from water-wave arrival times. These refined locations generally differ from deployment and recovery locations due to several factors, including the drift of the instrument while descending or ascending and uncertainty in the deployment/recovery ship's location. The orientation of each instrument on the sea floor was also computed from the horizontal polarization of water-wave arrivals, and was used to rotate the two horizontal components to transverse and radial directions. The rms error in water-wave arrival times ranged from 2 to 7 ms, which roughly translates to a location error in the direction of the seismic line of up to about 2 m when arrivals from at least 30 shots are used for the estimation. Likewise, the rms errors in water-wave polarization of less than 5 degrees for OBS stations 36, 37 and 39 and more than 10 degrees for rest of the stations correspond to instrument orientation errors of 1 and 2 degrees, respectively, for a 30-shot estimation.

Table 1. OBS Locations.

	Deployment Location	Water Depth(m)	Recovery Location	Water Depth(m)	Computed Location	Orientatio
34	22 °12.05'	3550	22 °11.86'	3550	22 °11.7156'	334.0
	121 °41.69'		121 °41.58'		121 °41.8896'	
35	22 °12.08'	950	22 °12.21'	1000	22 °11.9082'	243.6
	121 °30.00'		121 °29.85'		121 °30.2874'	
36	22 °12.07'	2730	22 °12.31'	2750	22 °11.7144'	121.7
	121 °21.37'		121 °21.24'		121 °21.393'	
37	22 °12.04'	994	22 °12.70'	900	22 °11.7174'	114.7
	121 °15.42'		121 °15.31'		121 °15.5994'	
38	22 °12.05'	1047	22 °12.46'	1000	22 °11.7456'	323.6
	121 °12.54'		121 °12.61'		121 °12.6702'	
39	22 °12.02'	1231	22 °12.14'	1250	22 °11.7456'	10.7
	121 °00.92'		121 °01.21'		121 °01.0518'	

The OBS SEG-Y data were debiased and then filtered with different band-passes to enhance shallow or deep events when needed. We also applied deconvolution to emphasize some of the shallow reflections. These processed data were then plotted in the form of record sections. The arrival picks used in this study were all made on vertical component record sections (Figure 3 and 4), while closely comparing the images from several different plots for the most appropriate selection of picks. The farthest arrival picks were at distances greater than 62 km for OBS 38, while on the seismic records of OBSs 35, 36 and 39 events were picked only within 30 km of each OBS because beyond this distance, arrivals were hardly discernible against background noise.

The arrival times picked from each OBS record section included those of near offset reflections, refractions and wide angle reflections from deeper layers. Arrival times were interpolated at a uniform spacing of 0.2 km to be used as input for the forward and inverse modeling (Zelt and Smith, 1992; Operto, 1996). The starting model was a simple structure consisting of six layers whose thickness increased generally from east to west along Line 29, since a transition from oceanic to arc-continental regime near the active margin of the Philippine Sea Plate is expected. The topography of the ocean bottom is based on our bathymetry log and DGPS data. A near-trace plot of the reflection profile confirms the bathymetry and offers some control over the thickness of the top layer of sedimentary rocks (Figure 5). The

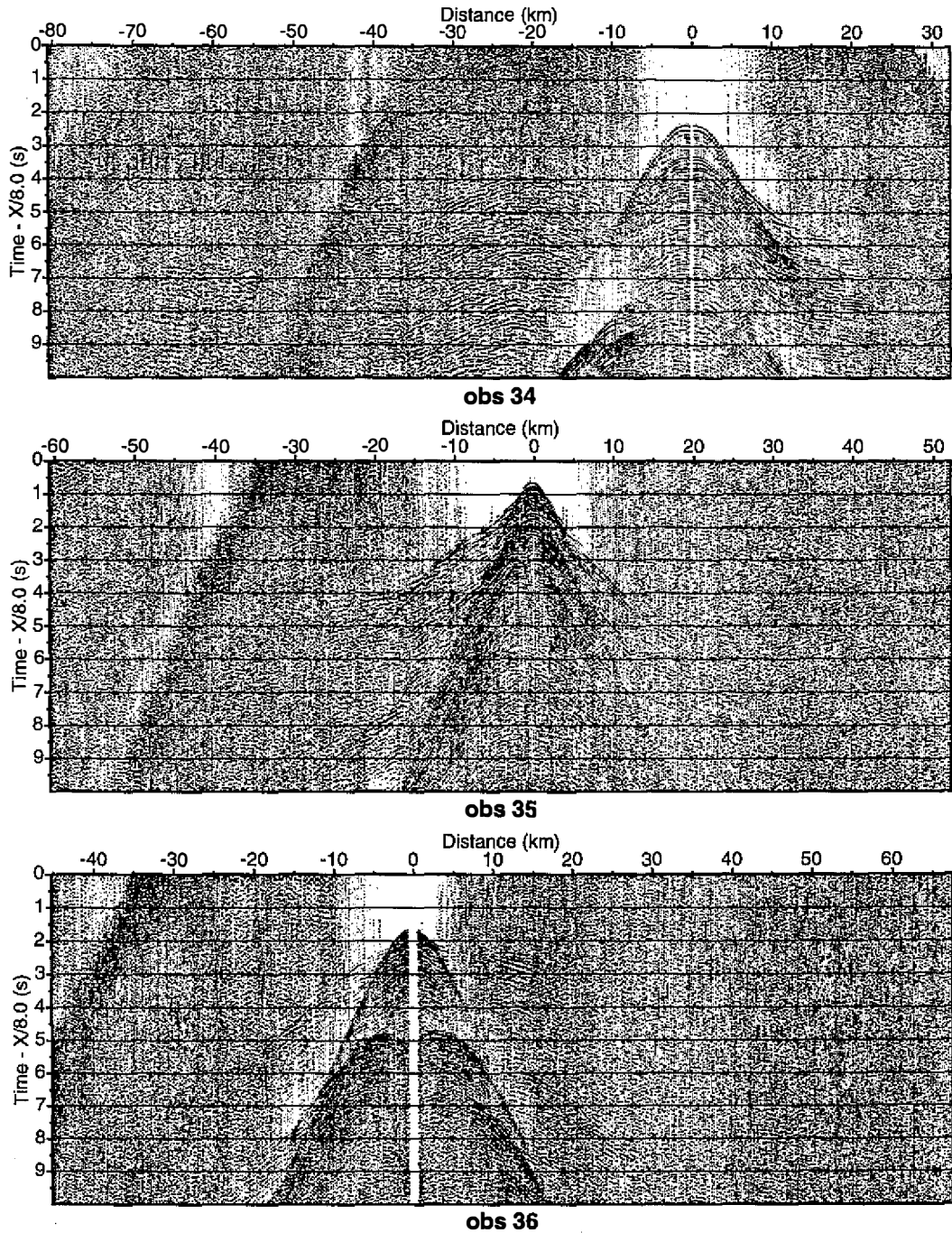
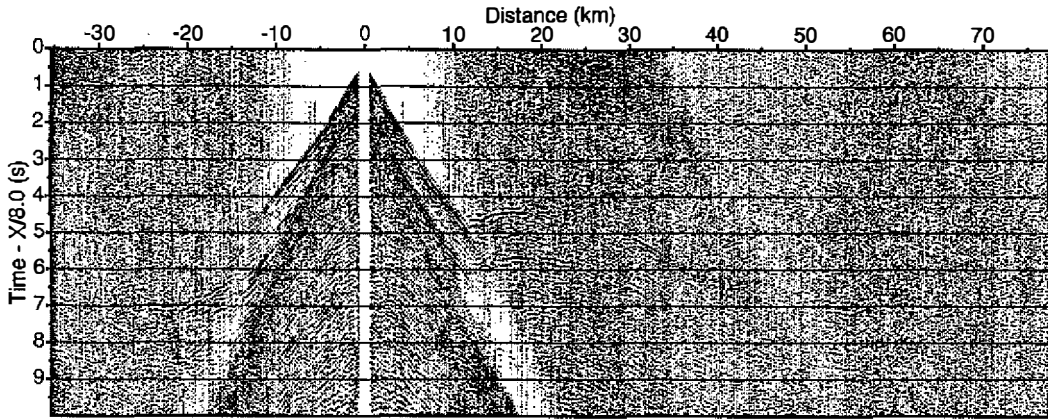
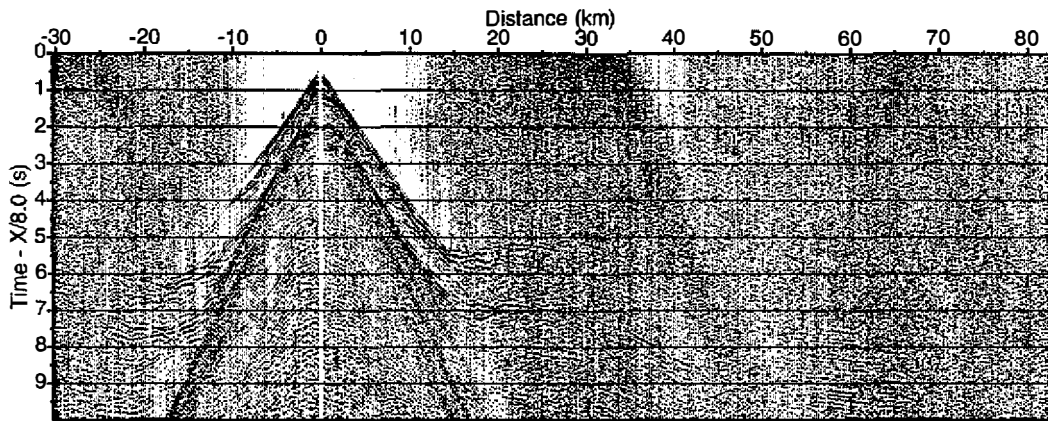


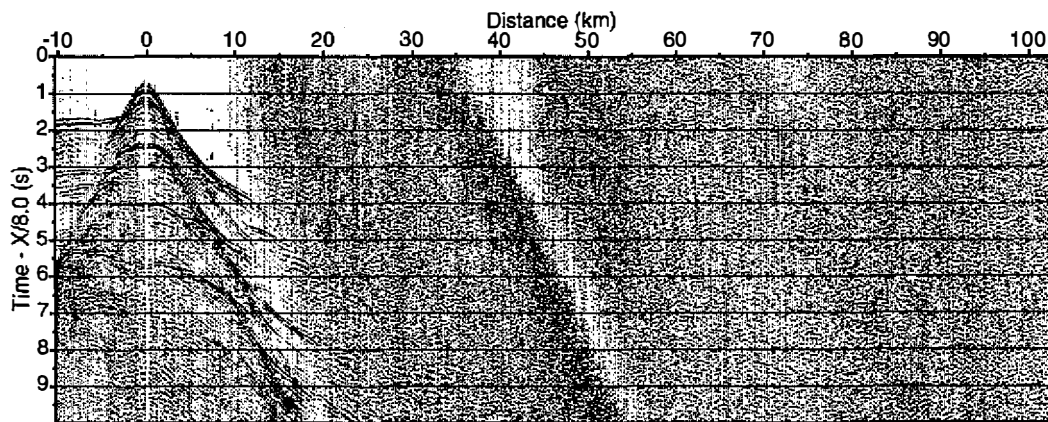
Fig. 3. Record sections (3-15 Hz) of vertical component of OBS 34-39 where OBS is located at 0 km mark and 8 km/sec velocity reduction is used.



obs 37



obs 38



obs 39

Fig. 3. (continued)

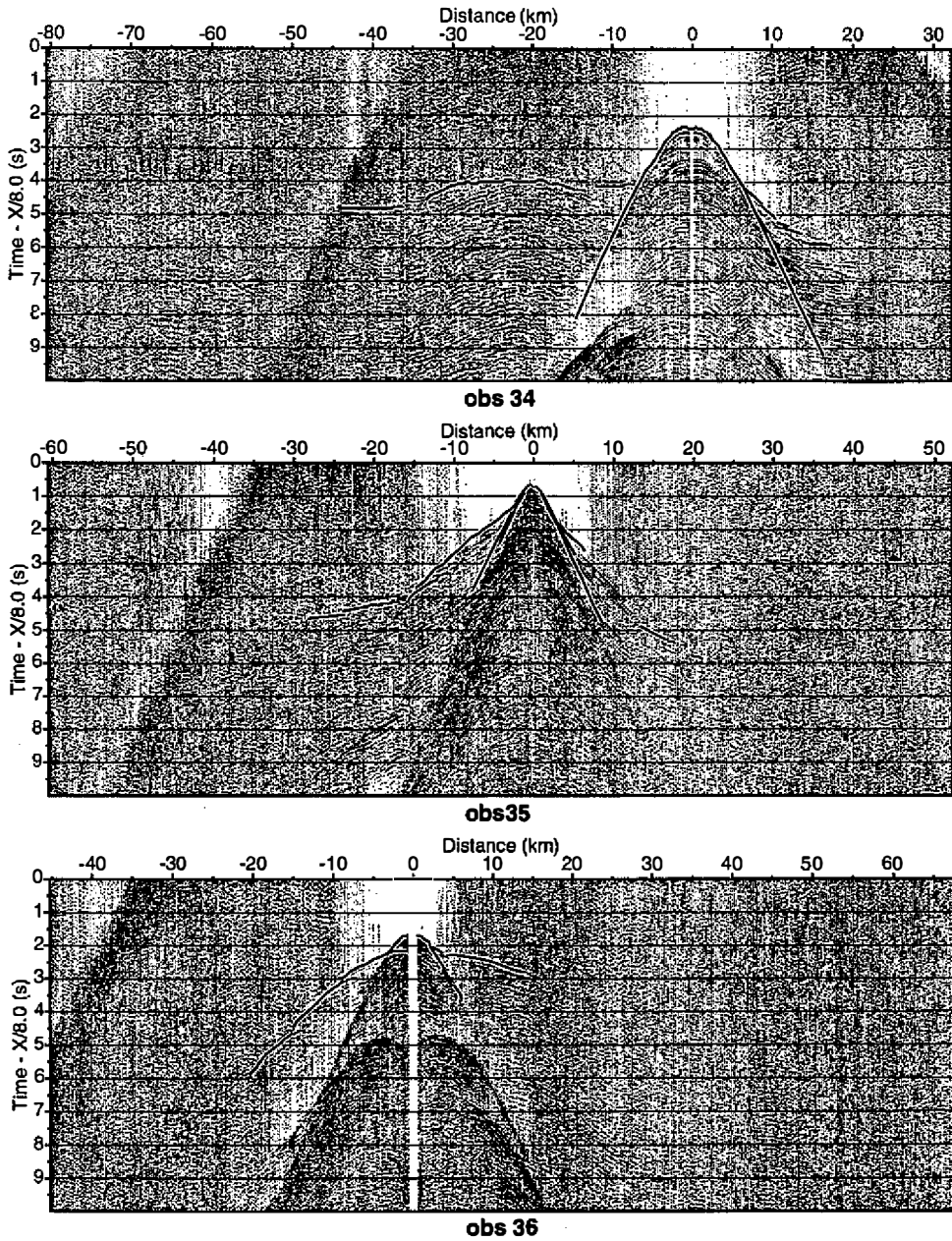
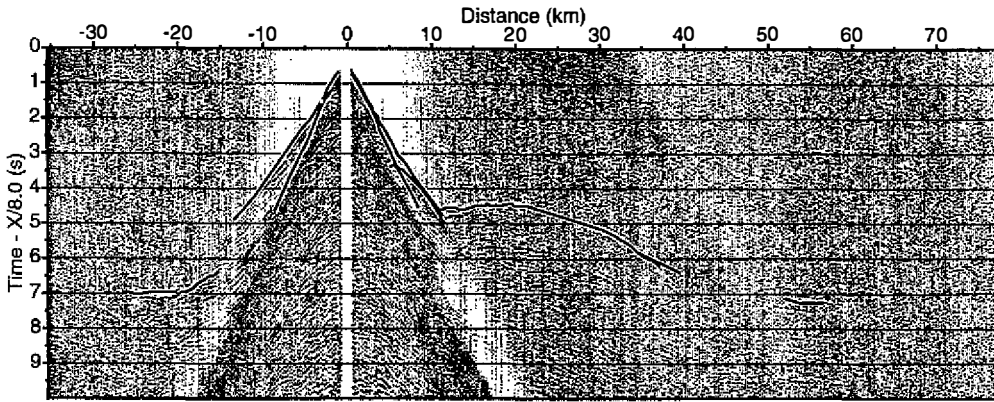
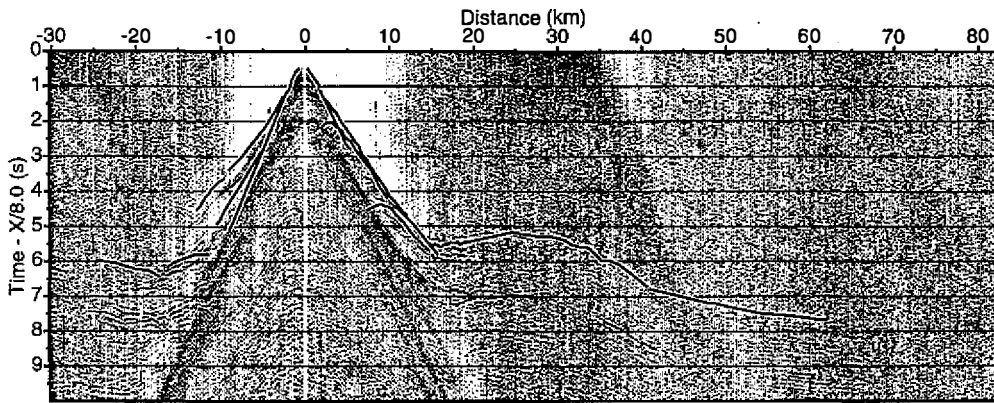


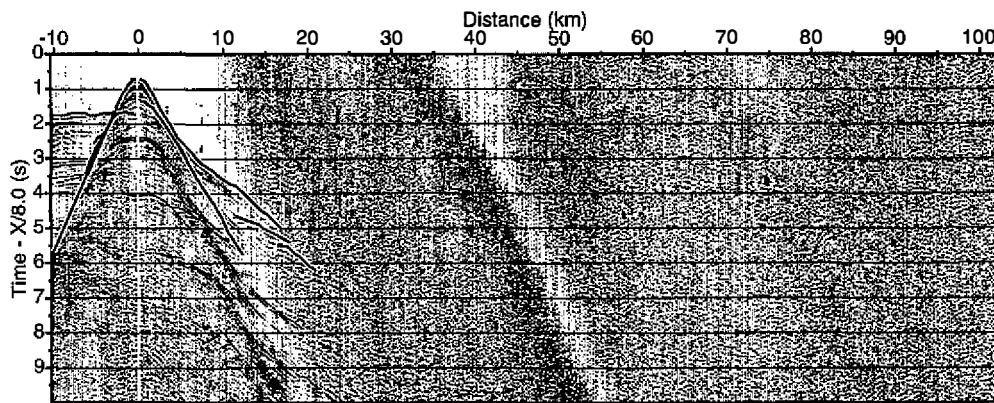
Fig. 4. As in Figure 3 with arrival picks superimposed. Note: arrival picks were mainly based on tracing troughs of first arrivals; some later arrivals were also picked if S/N was sufficiently high. Sometimes theoretical arrivals were compared to the picked curves to determine ray codes such as Pn, Pg, PmP, etc.



obs 37



obs 38



obs 39

Fig. 4. (continued)

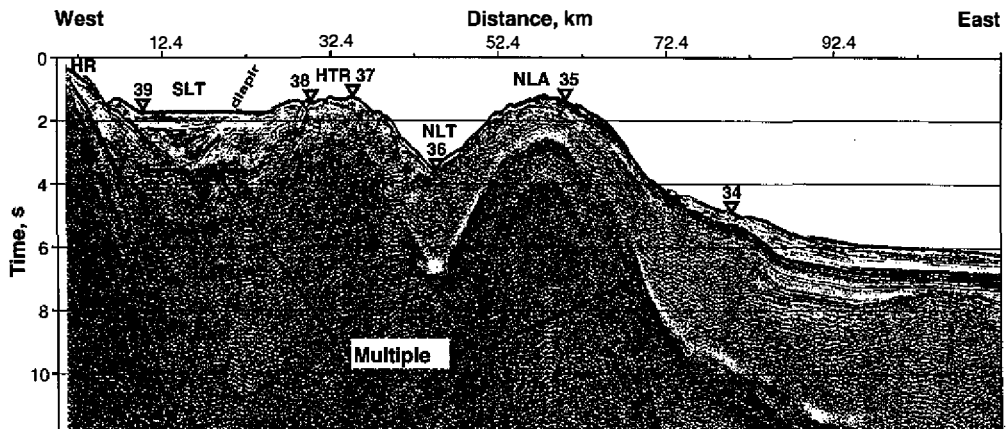


Fig. 5. CMP stack of multi-channel seismic data Line 29 (provided by Char-Shine Liu). Inverted triangles (V) indicate OBS locations. Note: a diastir can be seen near km 20.

ray inversion software developed by Zelt and Smith (1992) and later modified by Operto (1996) was used to compute the desired velocity model. A set of model parameters consisting of layer velocities and boundary depths was perturbed in order to improve the model for a better fit between the calculated and the observed times. The model was modified repeatedly until the rms travel time residual was reduced to less than 0.167 second. The final model we obtained and present here for discussion is a 6-layer model where the depth reaches below the Moho discontinuity (Figures 6 and 7).

5. RESULTS

The model generally exhibits westward thickening of the crust from a typical oceanic type, about 6 km thick, near the east end of the line, toward a continental type for the island, at least 15 km thick, near the coastline of Taiwan. However, we cannot rely on the model near both ends of the profile because of the unreversed nature of the ray paths. The detailed topography of the Moho discontinuity is also not well constrained since we were not able to pick a sufficient number of arrivals from this boundary for the inversion. The portion of the best resolution of the model is from km 10 to km 80 (*i.e.*, between OBSs 34 and 39).

The easternmost topographic high near km 56 corresponds to the Northern Luzon Arc, where sedimentary deposits are the thinnest, being less than 1 km thick. Moho beneath the topographic high is depressed to 17 km below sea level. The velocity within the lower crust here is about 6.5 km/sec, which is slower than elsewhere along the line.

Immediately west of the Northern Luzon Arc near km 45 is a topographic low, the North Luzon Trough. We find no significant sediments deposited within this topographic low as also illustrated in the MCS plot (Figure 5) (Lundberg, 1988). The thickness of the crust here,

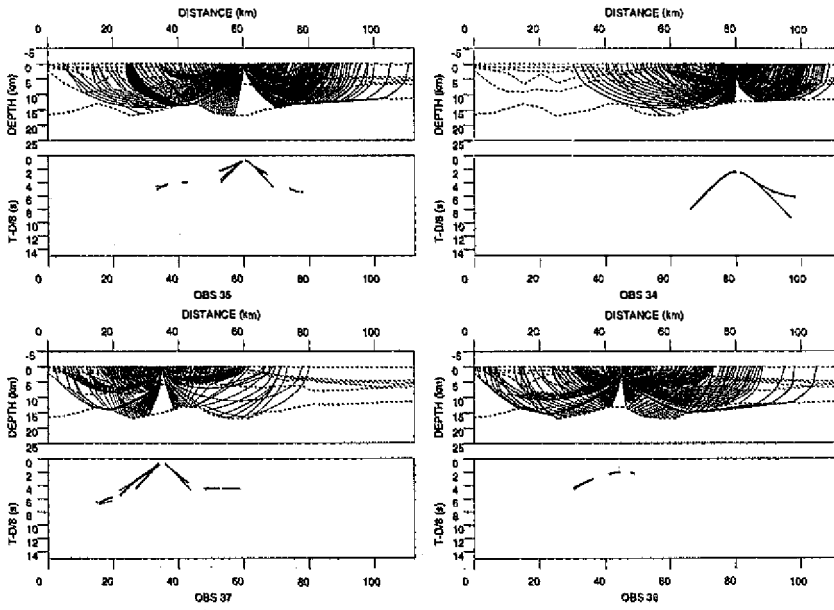


Fig. 6. The ray tracing of the final velocity model for each OBS and combined data with corresponding picked arrivals (thin curves) and calculated arrivals (thick curves) in each travel time diagram.

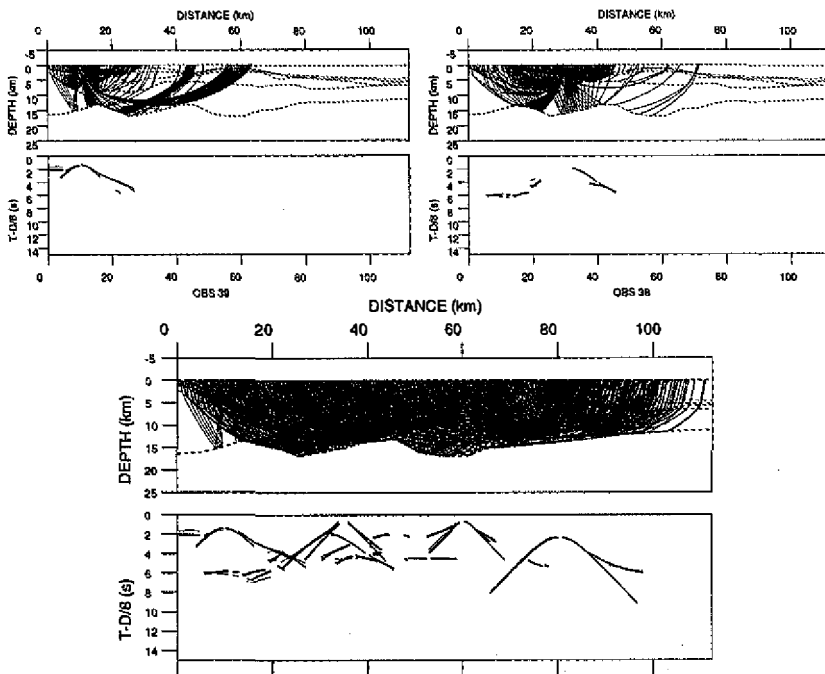


Fig. 6. (continued)

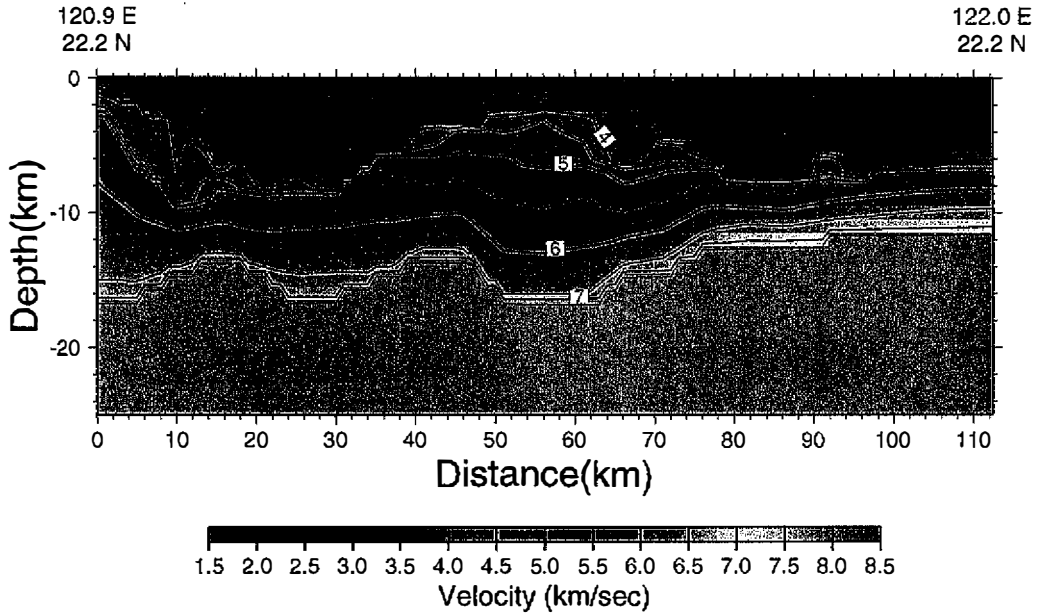


Fig. 7. The velocity contour profile of the final model.

in which the seismic velocity ranges from about 4 km/s to 6.6 km/s, is about 5 km less than that beneath the Northern Luzon Arc. The upper mantle is uplifted by about 3.5 km which can be seen by following the Moho velocity marks at 7.7-7.8 km/sec.

The crust thickens drastically again beneath the Huatung Ridge next to the North Luzon Trough. While the sea floor topography is shoaling, the depth to the lower boundary of the crust increases quickly to about 17 km. The bottom velocity of the thick crust reaches 6.85 km/s near km 25.

Farther west, the crust thins again rapidly, although the corresponding topographic depression is not apparent on the sea floor because of the thick cover of overlying sediments, the thickest part of which may reach 2.5 km or more. However, the crust may be about 3 km thinner here than beneath the Huatung Ridge and the structure may be more complex than can be resolved with our current velocity model. A small diapir may be present around the steepest slope along the lower sedimentary layer near km 20 as can also be seen on the MCS plot (Figure 5). This unique structure, whose geological significance is not clear, is beneath the Southern Longitudinal Trough, a trough that is on the offshore extension of the Taitung Longitudinal Valley and represents the suture zone of contact between the Taiwan block and the Philippine Sea Plate.

The deep crustal structure to the west of the Southern Longitudinal Trough is not clear because the survey line to the west of OBS 39, located at km 10, was too short for deeper refraction. Nonetheless, it is expected that the crust thickness increases greatly since the coastline of the Hengchun Peninsula is within 10 km of survey Line 29.

6. DISCUSSION

The arrival picks of the seismic records were by no means always clear and straightforward. Sometimes the arrivals we picked are based on very weak signals, and their accuracy is low. After many trials and checks of picked arrivals and repeated ray tracing, modeling and inversion, the velocity model that we obtained reveals some important features of which we have previously been unaware (Figure 7). The thick crust with the slowest velocity beneath the North Luzon Arc suggests that either the geotherm could be higher or the density lower under the volcanic ridge, than elsewhere along the line. Another zone of thick crust is found underneath the Huatung Ridge, an ancient subduction complex (Huang *et al.*, 1992) which has thickened to over 10 km as the Philippine Sea Plate continuously converges toward the Eurasian Plate. In addition, the North Luzon Trough and the Southern Longitudinal Trough, which are associated with a thin crust, can be interpreted as a forearc basin and the location of the ancient Manila Trench, respectively. An interesting difference between these two troughs is that while there is little sediment in the North Luzon Trough, at least a 2.5 km thickness of sediments has accumulated within the Southern Longitudinal Trough which is closer to the source of sediments.

Previous geophysical surveys provide some interesting results to which our model can be compared. The single-channel seismic reflection profiles collected from *R/V Chiu Lien* cruises in 1973 and 1975 showed a thick sediment package deposited in the Southern Longitudinal Trough (Bowin *et al.*, 1978; Huang *et al.*, 1992). The variation in magnetic anomaly is gentler away from the Northern Luzon Arc than along it (Bowin *et al.*, 1978; Shyu and Chen, 1991; Huang *et al.*, 1992; Liu *et al.*, 1992). More recent data from the cruises of *R/V Moana Wave* and *R/V Jean Charcot*, integrated with those previously acquired by *R/V Ocean Researcher I*, showed the Northern Luzon Arc to be associated with strong, positive anomalies (Liu *et al.*, 1992). Therefore, a shallower magnetic basement is expected along the volcanic arc, which may be related to the thickened crust beneath the topographic high near km 56 of our model. The free air gravity anomalies (FAAs) are closely correlated with the topographic highs and lows; thus, a positive FAA is associated with the Northern Luzon Arc, while negative FAAs are found where the troughs are located (Liu *et al.*, 1992; Yen *et al.*, 1995). The Bouguer gravity anomaly (BA) over the volcanic arc indicates the basement high while the basement low is related to the Huatung Ridge, a body of low density materials beneath the ocean floor (Huang *et al.*, 1992; Liu *et al.*, 1992). Finally, tomographic inversion of earthquake data can provide a valuable estimate of the three dimensional velocity structure. It is interesting to note that the Moho discontinuity at depths greater than 35 km suggested by such studies (Roecker *et al.*, 1987; Ma *et al.*, 1996) is much deeper than that suggested by our model within this study area. This difference may be due to the inaccuracy of tomographic determination outside the seismic station array.

There are two competing hypotheses as to where the boundary between the plates, the Philippine Sea Plate and the Eurasian Plate, lies in this area. One hypothesis places it along the Taitung Longitudinal Trough/Southern Longitudinal Trough, while the other, presented in a recent paper by Huang *et al.* (1997), places it further west, along the Lishan-Laonung-Hengchun fault. Our present results appear to support the former hypothesis.

The Philippine Sea Plate converges with the Eurasian Plate at a northwesterly speed of 7 cm/year and has been colliding with Taiwan along the Taitung Longitudinal Valley. In this process the Coastal Range was accreted at its frontal edge, while the continental margin has been pushed up at one of the highest uplift rates estimated for anywhere in the world (Karig, 1973; Karig and Sharman, 1975; Ho, 1982; Huang *et al.*, 1992). The collision started near Hualien and has been propagating toward the south while a clockwise rotation of the Luzon Volcanic Arc has been initiated as the Philippine Sea Plate continuously moves and shoves diagonally into the Asian continent (Lee *et al.*, 1991). The Luzon Volcanic Arc, whose northern part includes the Coastal Range, formed a typical arc-trench system with the ancient Manila Trench, which has since retreated southwestward from its former location near the Taitung Longitudinal Valley and the Southern Longitudinal Trough to its current position. The assumed arc-trench system can explain why there are two thin crustal structures in our velocity model corresponding to two troughs, the Taitung Trough/North Luzon Trough and the Taitung Longitudinal Valley/Southern Longitudinal Trough. This means that the Taitung Trough/North Luzon Trough was the forearc basin before the retreat of the ancient Manila Trench that existed along the Taitung Longitudinal Valley/Southern Longitudinal Trough and the Huatung Ridge is the former subduction complex of the ancient Luzon arc-trench system as evidenced by the deeply weathered sedimentary rocks and melange materials found in core samples (Huang *et al.*, 1992). Therefore, the Hengchun Peninsula was sitting to the west of an ancient trench before the modern Manila Trench was formed.

7. CONCLUSION

The offshore region east of the Hengchun Peninsula is the site where an arc-continent collision is underway. Based on velocity structure derived from OBS data, we find a thick crust beneath the Luzon Volcanic Arc, where seismic velocity on top of Moho discontinuity is the lowest along the profile. This low velocity may reflect a high geotherm within the arc. The 7 km-thick crust beneath the Southern Longitudinal Trough, the southern extension of Taitung Longitudinal Valley, is the thinnest in the model between OBS 34 and 39 and is the possible location of an ancient trench. The seismic structure is consistent with the concept that an ancient trench located at the suture zone has retreated further west.

Acknowledgments We thank K. McIntosh, T. K. Wang, and the crew of *M/V Maurice Ewing* and *R/V Ocean Researcher I* for their contribution of data acquisition. Char-Shine Liu served as the coordinator of the joint operation and provided the DGPS data for this work. University of Texas Institute for Geophysics provided some research facilities to one of the authors (ATC), and M. Wiederspahn and G. Christeson helped to set up the computing environment while ATC was visiting the institute. We appreciate K. McIntosh's comment in the discussion part and his help to improve the readability of the manuscript. We also benefit a lot from Anne Trehu and two anonymous reviewers critical comments and many editorial corrections. This project was supported by the National Science Council of the Republic of China under grant NSC 84-2611-M-019-011.

REFERENCES

- Angelier, J., H. T. Chu, and J. C. Lee, 1997: Shear concentration in a collision zone: Kinematics of the Chihshang Fault as revealed by outcrop-scale quantification of active faulting, Longitudinal Valley eastern Taiwan. *Tectonophys.*, **274**, 117-143.
- Biq, C. C., 1972: Dual-trench structure in the Taiwan-Luzon region. *Proc. Geol. Soc. China*, **15**, 65-75.
- Bowin, C., R. S. Lu, C. S. Lee, and H. S., 1978: Plate convergence and accretion in Taiwan-Luzon region. *Amer. Asso. Petrol. Geol. Bull.*, **62**, 1645-72.
- Chai, B. H. T., 1972: Structure and tectonic evolution of Taiwan. *Amer. Jour. Sci.*, **272**, 389-422.
- Chen, A. T., and Y. Nakamura, 1992: Investigating of deep crustal structure in the northeastern South China Sea and Taiwan Strait using ocean bottom seismographs. *Acta Geol. Taiwanica*, **30**, 145-148.
- Chen, A. T., Y. Nakamura, and L. W. Wu, 1994: Ocean Bottom Seismograph: instrumentation and experimental technique. *TAO*, **5**, 109-119.
- Chen, A. T., and Y. S. Jaw, 1996: Velocity structure near northern Manila Trench: an OBS refraction study. *TAO*, **3**, 277-297.
- Chen, W., 1991: Strain partition at oblique convergent plate boundaries: some implications on the kinematics of the Philippine Sea Plate and tectonics near Taiwan. Taicrust Workshop Proc., 199-208.
- Cheng, S. N., and Y. T. Yeh, 1991: Seismotectonics of the Taiwan-Luzon region as evidenced from seismicity and focal mechanism of earthquake. Taicrust Workshop Proc., 219-226.
- Christeson, G., 1995: OBSTOOL: software for processing UTIG OBS data. Univ. Texas Inst. Geophys. Tech. Rept., no. 134, 27 pp.
- Fuh, S. C., C. S. Liu, N. Lundberg, and D. L. Reed, 1997: Strike-slip fault offshore southern Taiwan: implications for the oblique arc-continent collision processes. *Tectonophys.*, **274**, 25-39.
- Henkart, P., 1990: SIOSEIS. Scripps Inst. Oceanography, Univ. of California.
- Ho, C. S., 1982: Tectonic evolution of Taiwan: explanatory text of the tectonic map of Taiwan. Ministry Economic Affairs, Taipei, Taiwan, 126 pp.
- Hu, J. C., J. Angelier, and S. B. Yu, 1997: An interpretation of the active deformation of southern Taiwan based on numerical simulation and GPS studies. *Tectonophys.*, **274**, 145-169.
- Huang, C. Y., C. T. Shyu, S. B. Lin, T. Q. Lee, and D. D. Sheu, 1992: Marine geology in the arc-continent collision zone off southeastern Taiwan: implications for Late Neogene evolution of the Coastal Range. *Marine Geology*, **107**, 183-212.
- Huang, C. Y., W. Y. Wu, C. P. Chang, S. Tsao, P. B. Yuan, C. W. Lin, and K. Y. Xia, 1997: Tectonic evolution of accretionary prism in the arc-continent collision terrace of Taiwan. *Tectonophys.*, **281**, 31-51.
- Karig, D. E., 1973: Plate convergence between the Philippines and the Ryukyu islands. *Mar.*

- Geol.*, **14**, 153-168.
- Karig, D. E., and G. F. Sharman, III, 1975: Subduction and accretion in trenches. *Geol. Soc. Amer. Bull.*, **86**, 377-389.
- Lee, J. C., J. Angelier, and H. T. Chu, 1997: Polyphase history and kinematics of a complex major fault zone in the northern Taiwan mountain belt: the Lishan Fault. *Tectonophys.*, **274**, 91-115.
- Lee, T. Q., C. Kissel, E. Barrier, C. Laj, and W. R. Chi, 1991: Paleomagnetic evidence for a diachronic clockwise rotation of the Coastal Range, eastern Taiwan. *Earth Planet. Sci. Lett.*, **104**, 245-257.
- Liu, C. S., S. Y. Liu, B. Y. Kuo, N. Lundberg, and D. Reed, 1992: Characteristics of the gravity and magnetic anomalies off southern Taiwan. *Acta Geol. Taiwanica*, **30**, 123-130.
- Lundberg, N., 1988: Present-day sediment transport paths south of the Longitudinal Valley, southeastern Taiwan. *Acta Geol. Taiwanica*, **26**, 317-331.
- Ma, K. F., J. H. Wang, and D. Zhao, 1996: Three-dimensional seismic velocity structure of the crust and uppermost mantle beneath Taiwan. *J. Phys. Earth*, **44**, 85-105.
- Nakamura, Y., 1994: Suggested basic processing procedures for UTIG OBS data from artificial sources. Univ. Texas Inst. Geophys. Tech. Rept., no. 129, 38 pp.
- Nakamura, Y., and J. Garmany, 1991: Development of upgraded ocean-bottom seismograph. Univ. Texas Inst. Geophys. Tech. Rept., no. 111, 45 pp.
- Nakamura, Y., K. McIntosh, and A. T. Chen, 1998: Preliminary results of a large offset seismic survey west of Hengchun Peninsula, southern Taiwan. *TAO*, **9**, 395-408.
- Operto, S., 1996: RSTTI package: ray base seismic travel time inversion. Univ. Texas Inst. Geophys. Tech. Rept., no. 148, 40 pp.
- Roecker, S. W., Y. H. Yeh and Y. B. Tsai, 1987: Three-dimensional P and S wave velocity structures beneath Taiwan: deep structure beneath an arc-continent collision. *J. Geophys. Res.*, **92**, 10547-570.
- Rau, R. J., and F. T. Wu, 1995: Tomographic imaging of lithospheric structures under Taiwan. *Earth Planet. Sci. Lett.*, **133**, 517-532.
- Shyu, C. T., and S. C. Chen, 1991: A topographic and magnetic analysis off southeastern Taiwan. *Acta Oceanog. Taiwanica*, **27**, 1-20.
- Teng, L. S., 1991: Geology of Taiwan in tectonic framework of arc-continent collision. Taicrust Workshop Proc., 63-73.
- Yen, H. Y., W. T. Liang, B. Y. Kuo, Y. H. Yeh, C. S. Liu, D. Reed, N. Lundberg, F. C. Su, and H.S. Chung, 1995: A regional gravity map for the subduction-collision zone near Taiwan. *TAO*, **6**, 233-250.
- Yu, S. B., H. Y. Chen, and L. C. Kuo, 1997: Velocity field of GPS stations in the Taiwan area, *Tectonophys.*, **274**, 41-59.
- Zelt, C. A., and R. B. Smith, 1992: Seismic traveltimes inversion for 2-D crustal velocity structure. *Geophys. J. International*, **108**, 16-34.